THE JOURNAL OF PHYSICAL CHEMISTRY C

Article

pubs.acs.org/JPCC

Aqueous, Heterogeneous *para*-Hydrogen-Induced ^{15}N Polarization

Liana B. Bales,[†] Kirill V. Kovtunov,*[,‡,§] Danila A. Barskiy,[○] Roman V. Shchepin,[○] Aaron M. Coffey,[○] Larisa M. Kovtunova,[§,∥] Andrey V. Bukhtiyarov,[∥] Matthew A. Feldman,[○] Valerii I. Bukhtiyarov,[§,∥] Eduard Y. Chekmenev,*[,⊥,#,○] Igor V. Koptyug,[‡,§] and Boyd M. Goodson*[,†,▽]

[†]Department of Chemistry and Biochemistry, and [▽]Materials Technology Center, Southern Illinois University, Carbondale, Illinois 62901, United States

[‡]International Tomography Center SB RAS, Novosibirsk 630090, Russia

[§]Novosibirsk State University, Novosibirsk 630090, Russia

[∥]Boreskov Institute of Catalysis SB RAS, Novosibirsk 630090, Russia

[⊥]Department of Biomedical Engineering and Physics, Vanderbilt-Ingram Cancer Center (VICC), and [○]Vanderbilt Institute of Imaging Science (VUIIS), Department of Radiology, Vanderbilt University Medical Center, Nashville, Tennessee 37232, United States

[#]Russian Academy of Sciences, Moscow 119991, Russia

Supporting Information

ABSTRACT: The successful transfer of *para*-hydrogen-induced polarization to ^{15}N spins using heterogeneous catalysts in aqueous solutions was demonstrated. Hydrogenation of a synthesized unsaturated ^{15}N-labeled precursor (neurine) with *para*hydrogen (p-H_2) over Rh/TiO_2 heterogeneous catalysts yielded a hyperpolarized structural analogue of choline. As a result, ^{15}N polarization enhancements of over 2 orders of magnitude were achieved for the ^{15}*N*-labeled ethyltrimethylammonium ion product in deuterated water at elevated temperatures. Enhanced ^{15}N NMR spectra were successfully acquired at 9.4 and 0.05 T. Importantly, long hyperpolarization lifetimes were observed at 9.4 T, with a ^{15}N T_1 of ∼6 min for the product molecules, and the T_1 of the deuterated form exceeded 8 min. Taken together, these results show that this approach for generating hyperpolarized species with extended lifetimes in aqueous, biologically compatible solutions is promising for various biomedical applications.

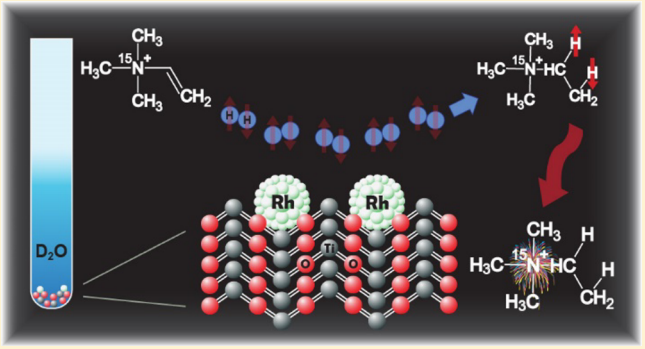

INTRODUCTION

Hyperpolarization—the creation of highly nonequilibrium nuclear spin polarization—has been investigated for years as a way to dramatically improve the detection sensitivity of NMR and MRI.[1−8] Although many hyperpolarization methods have been developed, dissolution dynamic nuclear polarization (d-DNP)[9,10] has become increasingly dominant for biomedical applications because of advanced technology enabling the preparation of hyperpolarized (HP) nuclear spins within a wide range of chemical and biological systems, including metabolic MRI contrast agents now under investigation in clinical trials.[11−13] However, the high costs and infrastructure associated with d-DNP technology, combined with relatively slow production rates, present a challenge for many potential applications.

Approaches exploiting *para*-hydrogen-induced polarization (PHIP)[14−17] could be attractive alternatives because of their dramatically lower costs and instrumentation demands, much greater hyperpolarization rates (minutes to seconds, even allowing continuous agent production), and potential for scalability. In "traditional" PHIP,[15,18] the pure spin order from *para*hydrogen (p-H_2) gas is transferred to a molecular substrate via the pairwise hydrogenation of asymmetric unsaturated bonds, a process that is typically facilitated with a catalyst. Key recent PHIP developments for biomedical applications include the demonstration of PHIP in aqueous media[19−25] and PHIP using heterogeneous catalysts (HET-PHIP).[26−30] The latter approach enables facile separation of the catalyst from the target molecule and, hence, the potential preparation of "pure" HP agents and catalyst reuse. However, also of great importance is the transfer of spin order from the nascent protons to substrate heteronuclei (e.g., ^{13}C), providing greater hyperpolarization lifetimes compared to ^{1}H spins. ^{13}C hyperpolarization via PHIP has been achieved via both RF-driven polarization transfer[31−36] and polarization transfer in a magnetic shield (i.e., field cycling),[37,38] an approach that very

Received: June 16, 2017
Revised: June 20, 2017
Published: June 21, 2017

DOI: 10.1021/acs.jpcc.7b05912
J. Phys. Chem. C 2017, 121, 15304−15309

recently has been extended to HET-PHIP conditions to produce aqueous solutions of highly polarized ^{13}C-containing molecules free from the catalyst.[27,39]

Translation of this approach to ^{15}N spins could have many advantages; indeed, Aime and co-workers have recently demonstrated ^{15}N hyperpolarization of propargylcholine-^{15}N via homogeneous PHIP and field cycling in a mixture of acetone and methanol or in water.[40] In addition to greatly increasing agent diversity, agents with HP ^{15}N spins can be spectrally sensitive to the local biochemical environment.[41−43] Importantly, ^{15}N T_1 values are often considerably longer than corresponding ^{13}C values,[43−45] thereby enabling longer hyperpolarization storage (either for direct readout or for transfer to ^{1}H for more sensitive detection);[46−52] such T_1 values are expected to be even longer at lower magnetic fields.[53,54]

Herein, we report ^{15}N NMR hyperpolarization of a structural analogue of choline via heterogeneous, aqueous-phase hydrogenation of ^{15}N-trimethyl(vinyl)-ammonium (i.e., neurine-^{15}N) bromide over solid Rh/TiO$_2$ catalysts. The PHIP-derived ^{15}N nuclear spin polarization achieved in these experiments is the first reported to date involving heterogeneous catalysis and yielded ^{15}N enhancements of $\sim 2 \times 10^2$-fold and a long relaxation time of ~350 s at 9.4 T; deuterating the substrate yielded weaker enhancements but a longer relaxation time (^{15}N $T_1 \approx 500$ s). Finally, significant signal enhancement is shown for the first time to enable detection at low (0.05 T)[55] magnetic field of the ^{15}N resonance for molecules polarized using PHIP. For most of the heterogeneous hydrogenation reactions in this work, hydrogen gas was used with 50% p-H$_2$ enrichment (the normal room-temperature ratio of *para*- to *ortho*-hydrogen is 25/75) prepared with a home-built generator (more details concerning experiments, chemical synthesis, and characterization are provided in the Supporting Information (SI)).

RESULTS AND DISCUSSION

In one experiment, freshly produced p-H$_2$ was bubbled at 90 psi into a medium-wall NMR tube (using a previously developed setup)[27,39] containing the target substrate (neurine-^{15}N bromide) and the heterogeneous catalyst Rh/TiO$_2$ in water (D$_2$O) at 90 °C, causing the unsaturated substrate to be hydrogenated via pairwise addition. The reaction was performed under ALTADENA[56] conditions (i.e., wherein the hydrogenation reaction was performed outside of the magnet at low field), and results are shown in Figure 1 (see also Figures S5 and S8). In order to effect the transfer of spin order from nascent ^{1}H substrate spins to ^{15}N, the hydrogenation reaction was performed by using a magnetic shield, similar to the recently reported procedure—also know as the magnetic field cycling (MFC) approach,[27,57−59] but in our case, the hydrogenation reaction was carried out directly in the magnetic shield. The level of polarization achieved is strongly dependent upon the speed of the sample transfer from the low (micro-Tesla) field to the Earth's field;[40] therefore, to avoid related issues, the hydrogenation reaction was performed directly in the magnetic shield, and only after the termination of p-H$_2$ bubbling was the sample quickly transferred to the high-field NMR for analysis. A strong ^{15}N NMR signal was observed for the HP product (Figure 1B); however, no ^{15}N signal was observed prior to p-H$_2$ bubbling (Figure 1A).

This ^{15}N NMR enhancement was achieved using Rh/TiO$_2$ catalyst with 1.0% Rh loading. Importantly, utilization of Rh/TiO$_2$ solid catalyst for heterogeneous PHIP[60,61] can, in principle, allow one to alter the conversion rate by varying

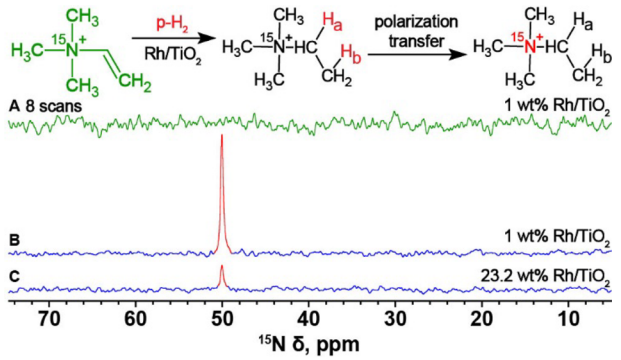

Figure 1. (A) ^{15}N NMR spectrum of a 0.25 M ^{15}N-neurine substrate in the presence of 1.0% Rh/TiO$_2$ before reaction with p-H$_2$ in D$_2$O, recorded with eight scans and a 30 s repetition delay; no signal of reactant is observed at 58 ppm under these conditions. ^{15}N NMR spectrum of the hyperpolarized product using the same acquisition parameters as those used for spectrum acquisition shown in (A) but taken with 1 scan after transfer of spin order to ^{15}N, achieved with 30 s 50%-enriched p-H$_2$ bubbling inside of the magnetic shield. (C) Same as (B) but with hydrogenation occurring over 23.2% Rh/TiO$_2$. HP ^{15}N spectra are shown with an absorptive phase (i.e., sharing the same phase as a thermally polarized ^{15}N sample); note that the field cycling was not optimized for polarization transfer.

the Rh fraction[62] of the catalytic material without decreasing the achieved polarization level of the products.[27] To investigate this possibility for the present reaction, a second Rh/TiO$_2$ catalyst with 23.2% Rh loading was also used (Figure 1C). Although an enhanced ^{15}N signal of the product is observed with the 23.2% Rh/TiO$_2$ catalyst, the signal is ~3.7-fold weaker than that observed with the 1.0% Rh catalyst. The explanation comes from the corresponding ^{1}H HET-PHIP spectra (Figure S8), which indicate that, while the 23.2% Rh catalyst does indeed yield much higher reaction rates (in fact, providing essentially complete conversion of the substrate in 30 s), a smaller ^{1}H polarization enhancement is achieved, giving rise to the weaker ^{15}N enhancement in Figure 1 (possibly reflecting either reduced pairwise H$_2$ addition or different ^{1}H relaxation of species adsorbed onto catalyst particles). Thus, the 1.0% Rh catalyst was used for the subsequent experiments in this work. In any case, these observations are the first reported to date for hyperpolarization of ^{15}N-containing molecules via heterogeneous catalysis with ^{15}N polarization derived from the spin order from p-H$_2$.

The effects of substrate deuteration and increased p-H$_2$ fraction on ^{15}N signal enhancement were also separately investigated. Deuteration has previously been shown to increase heteronuclear (e.g., ^{13}C) T_1 in the context of PHIP[63,64] and DNP.[65] Here, following successful observation of ^{1}H HET-PHIP with the fully deuterated substrate (neurine-^{15}N-d_{12} bromide; see the SI for synthesis and Figure S9 for spectra), the approach described above was used to demonstrate ^{15}N enhancement of the product in the aqueous phase following heterogeneous hydrogenation (Figure 2A). However, the intensity of this ^{15}N line was slightly lower than that of the fully protonated substrate studied under the same conditions (Figure 2B). This reduced ^{15}N enhancement with deuterated substrates is analogous to that observed with ^{15}N SABRE-SHEATH (Signal Amplification By Reversible Exchange in SHield Enables Alignment to Heteronuclei)[66] and likely reflects either enhanced ^{15}N relaxation in the μT regime (i.e. within the

DOI: 10.1021/acs.jpcc.7b05912
J. Phys. Chem. C 2017, 121, 15304−15309

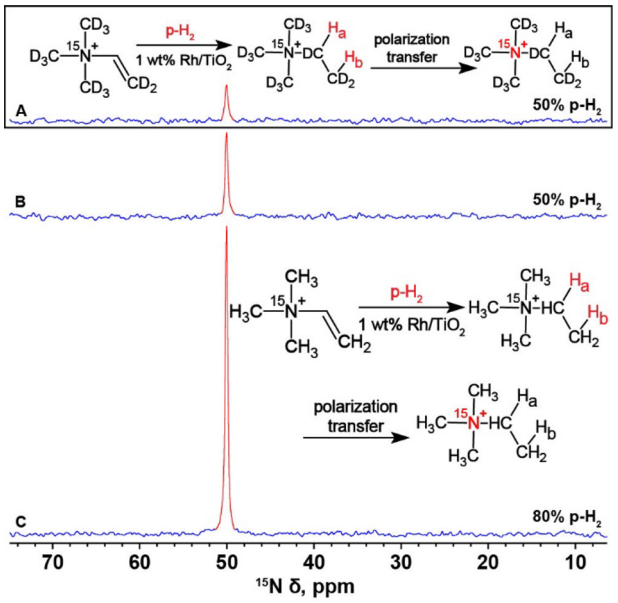

Figure 2. (A) Single-shot ^{15}N NMR spectrum of the fully deuterated substrate (0.125 M) solution in D_2O obtained after 30 s of *p*-H_2 bubbling (50% *p*-H_2 fraction) and polarization transfer to ^{15}N using the magnetic shield. (B) Same as (A) but with the protonated substrate (0.125 M). (C) Same as (B) but with an 80% *p*-H_2 fraction.

magnetic shield) or a more direct loss of spin order into the ^{2}H spin degrees of freedom under those conditions.

On the other hand, use of a greater *p*-H_2 fraction with the protonated substrate did yield an expected increase in ^{15}N signal enhancement (Figure 2C). For this experiment, the *p*-H_2 fraction was increased to 80% using a cryocooler-based *p*-H_2 generator operating at a temperature lower than the 77 K of lN_2 (see the SI for details). Increasing the ratio of *para*- to *ortho*-H_2 from ∼50/50 (Figure 2B) to ∼80/20 (Figure 2C) yielded an improvement in the product's ^{15}N signal enhancement by nearly 3-fold, approaching the full 3-fold increase that would be theoretically expected if 100% *p*-H_2 had been used. Taking the results from Figures 1 and 2 together, the greatest signal enhancement was achieved using 80% *p*-H_2 on the protonated substrate in the presence of 1.0% Rh/TiO_2.

In PHIP, quantification of the sensitivity gain provided by the polarization level requires not only comparison with a signal from a thermally polarized sample but also an estimation of the efficiency of the hydrogenation reaction (and hence, the concentration of the product) at the time of detection. Here, the HP ^{15}N signal was compared to the thermally polarized signal obtained from a 3.2 M $^{15}NH_4Cl$ aqueous solution. Note that the spectrum in Figure 2C was obtained after the first 30 s of *p*-H_2 bubbling; comparison with thermal ^{15}N (and ^{1}H) spectra obtained with different bubbling times allowed the conversion level of the reagent to the product to be estimated at ∼10% (see Figure S10C). Therefore, the concentration of the product in Figure 2C is approximately 0.0125 M, yielding a corresponding ^{15}N signal enhancement of $\varepsilon \approx 2 \times 10^2$ (attempts to detect polarization of ^{15}N nuclei at natural abundance were unsuccessful).

While the ^{15}N signal increased steadily with *p*-H_2 bubbling time for the first 30 s of reaction, after that point, the signal tended to level off until the hydrogenation reaction yield reached 100% (not shown). This behavior could be potentially explained by changes in relaxation of species adsorbed onto the catalyst particles. Importantly, the ^{15}N hyperpolarization was found to be long-lived at 9.4 T for both the protonated and deuterated substrates, with T_1 decay constants of 348 ± 10 and 494 ± 13 s, respectively (Figure 3), values that are roughly 1−2

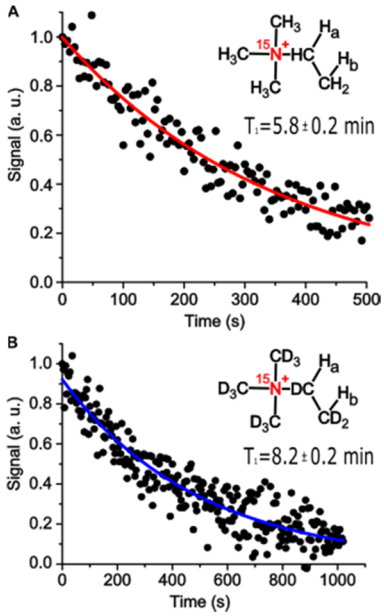

Figure 3. HP ^{15}N T_1 relaxation curves measured at 9.4 T for the protonated (A) and deuterated product (B); curves are exponential fits, giving the ^{15}N T_1 values (not corrected for ∼10° tipping-angle pulses) and error margins. Note the >2-fold time axis scale difference.

orders of magnitude longer that the corresponding lifetimes of ^{1}H hyperpolarization and a factor of 2 larger than that recently reported for ^{15}N derivatives of choline.[40]

Finally, because the magnetization of HP species is not endowed by the NMR/MRI magnet, in principle, strong magnets are not required for detection. To investigate the feasibility of performing low-field NMR/MRI with ^{15}N spins hyperpolarized by HET-PHIP, hydrogenation reaction products for both protonated and deuterated substrates were detected at 0.05 T, Figure 4. Indeed, ^{15}N NMR resonances were successfully detected via low-field ^{15}N NMR spectroscopy at a 210 kHz resonance frequency, with slightly greater signal observed for the protonated versus the deuterated product, which is qualitatively consistent with the high-field results. Higher polarization enhancements enabled by future experimental refinements should boost the signal to noise ratio to allow measurement of the ^{15}N T_1 at low field, where even longer hyperpolarization lifetimes would be expected,[54] thereby improving storage of the HP state.

CONCLUSIONS

In summary, heterogeneous Rh/TiO_2 catalysts and MFC were used to achieve ^{15}N hyperpolarization via HET-PHIP for the first time; previous transfers of spin order from *p*-H_2 to ^{15}N spins had only been achieved under homogeneous catalytic conditions via PHIP/MFC[40] or SABRE-SHEATH.[67,68] ^{15}N nuclear spin polarization enhancements of ∼2×10^2 fold (at 9.4 T) were observed in aqueous solutions following hydrogenation of neurine-^{15}N bromide with *p*-H_2, which yielded a structural analogue of the biological molecule choline (the HP form of which has been shown promising in vivo[45] because of

DOI: 10.1021/acs.jpcc.7b05912
J. Phys. Chem. C 2017, 121, 15304−15309

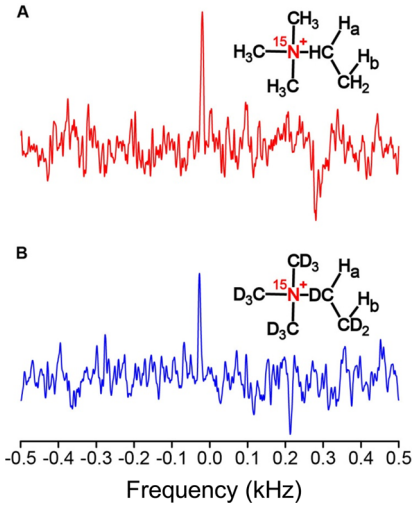

Figure 4. Single-shot low-field (0.05 T) HP ^{15}N NMR spectra of (A) the fully protonated product and (B) the fully deuterated product obtained via heterogeneous hydrogenation of neurine-^{15}N bromide over a 1.0% Rh/TiO_2 catalyst with 80% p-H_2. Peaks of interest are at an offset of ∼(−)0.025 kHz.

the widespread function of choline in cellular metabolism and its significantly upregulated metabolism in cancer).[69,70] Larger enhancements were observed with 1.0 versus 23.2% Rh/TiO_2 as well as with higher p-H_2 fractions; however, deuteration of the substrate yielded lower enhancements but a longer hyperpolarization lifetime. Indeed, very long ^{15}N T_1 values were observed at 9.4 T for both the protonated and deuterated substrates, ∼6 and >8 min, respectively. The ^{15}N hyperpolarization via HET-PHIP also enabled observation of ^{15}N signals at low (0.05 T) field, where even longer hyperpolarization lifetimes are expected, further demonstrating the potential for wider applicability of the approach. Moreover, these results also expand the range of molecules (including biomolecules) amenable to HET-PHIP hyperpolarization. While the molecule hyperpolarized here lacks the −OH moiety found in choline, PHIP precursors for choline hyperpolarization have been previously described.[71] It should also be noted that the heterogeneous catalysts used (Rh/TiO_2) are very stable and do not undergo any modifications during reaction (as was confirmed by XPS analysis; see the SI). Therefore, the absence of leaching of the active component of the catalyst material into solution, combined with the ability to use such supported metal catalysts for aqueous-phase heterogeneous hydrogenation (given their potential for facile separation), should allow not only catalyst recycling and reuse but also the preparation of pure HP substances free from the presence of the catalyst. Although the reported polarization values need to be increased further, taken together, these results open a door to the rapid and inexpensive creation of pure agents with long hyperpolarization lifetimes for various biomedical applications, including in vivo molecular MR imaging.

■ ASSOCIATED CONTENT

Supporting Information

The Supporting Information is available free of charge on the ACS Publications website at DOI: 10.1021/acs.jpcc.7b05912.

Experimental procedures, synthesis of protonated and deuterated substrate molecules, catalyst synthesis, catalyst characterization (before and after hydrogenation reaction), and additional figures (PDF)

■ AUTHOR INFORMATION

Corresponding Authors

*E-mail: kovtunov@tomo.nsc.ru (K.V.K.).
*E-mail: eduard.chekmenev@vanderbilt.edu (E.Y.C.).
*E-mail: bgoodson@chem.siu.edu (B.M.G.).

ORCID

Kirill V. Kovtunov: 0000-0001-7577-9619
Danila A. Barskiy: 0000-0002-2819-7584
Andrey V. Bukhtiyarov: 0000-0002-0199-8111
Eduard Y. Chekmenev: 0000-0002-8745-8801
Igor V. Koptyug: 0000-0003-3480-7649
Boyd M. Goodson: 0000-0001-6079-5077

Notes

The authors declare no competing financial interest.

■ ACKNOWLEDGMENTS

We thank NSF (CHE-1416432, CHE-1416268, and REU DMR-1461255), NIH (1R21EB018014, 5R00CA134749, 5R00CA134749-02S1, and 1R21EB020323), and DoD (CDMRP BRP W81XWH-12-1-0159/BC112431, PRMRP W81XWH-15-1-0271, and W81XWH-15-1-0272). I.V.K., V.I.B., and K.V.K. thank RFBR (17-54-33037 and 16-03-00407-a), MK-4498.2016.3, and FASO Russia Project # 0333-2016-0001 for basic funding. B.M.G. and A.M.C. acknowledge the SIUC MTC and NIH 1F32EB021840. L.M.K. thanks SB RAS Integrated Program of Fundamental Scientific Research No. II.2 (No. 0303-2015-0010) for catalyst preparation. The BIC team thanks RSCF (Grant #14-23- 00146).

■ REFERENCES

(1) Green, R. A.; Adams, R. W.; Duckett, S. B.; Mewis, R. E.; Williamson, D. C.; Green, G. G. R. The Theory and Practice of Hyperpolarization in Magnetic Resonance Using Parahydrogen. *Prog. Nucl. Magn. Reson. Spectrosc.* **2012**, *67*, 1−48.
(2) Nikolaou, P.; Goodson, B. M.; Chekmenev, E. Y. NMR Hyperpolarization Techniques for Biomedicine. *Chem. - Eur. J.* **2015**, *21*, 3156−3166.
(3) Bowers, C. R. Sensitivity Enhancement Utilizing Parahydrogen. *Encycl. Magn. Reson.* **2007**, *9*, 4365−4384.
(4) Barskiy, D. A.; Coffey, A. M.; Nikolaou, P.; Mikhaylov, D. M.; Goodson, B. M.; Branca, R. T.; Lu, G. J.; Shapiro, M. G.; Telkki, V.; Zhivonitko, V. V.; et al. NMR Hyperpolarization Techniques of Gases. *Chem. - Eur. J.* **2017**, *23*, 725−751.
(5) Koptyug, I. V. Spin Hyperpolarization in NMR to Address Enzymatic Processes in Vivo. *Mendeleev Commun.* **2013**, *23*, 299−312.
(6) Goodson, B. M. Nuclear Magnetic Resonance of Laser-Polarized Noble Gases in Molecules, Materials, and Organisms. *J. Magn. Reson.* **2002**, *155*, 157−216.
(7) Brindle, K. M. Imaging Metabolism with Hyperpolarized ^{13}C-Labeled Cell Substrates. *J. Am. Chem. Soc.* **2015**, *137*, 6418−6427.
(8) Schroder, L. Xenon for NMR Biosensing - Inert but Alert. *Phys. Medica* **2013**, *29*, 3−16.
(9) Ardenkjaer-Larsen, J. H.; Fridlund, B.; Gram, A.; Hansson, G.; Hansson, L.; Lerche, M. H.; Servin, R.; Thaning, M.; Golman, K. Increase in Signal-to-Noise Ratio of > 10,000 Times in Liquid-State NMR. *Proc. Natl. Acad. Sci. U. S. A.* **2003**, *100*, 10158−10163.
(10) Maly, T.; Debelouchina, G. T.; Bajaj, V. S.; Hu, K.-N.; Joo, C.-G.; Mak-Jurkauskas, M. L.; Sirigiri, J. R.; van der Wel, P. C. A.; Herzfeld, J.; Temkin, R. J.; et al. Dynamic Nuclear Polarization at High Magnetic Fields. *J. Chem. Phys.* **2008**, *128*, 052211.

DOI: 10.1021/acs.jpcc.7b05912
J. Phys. Chem. C 2017, 121, 15304−15309

(11) Nelson, S. J.; Kurhanewicz, J.; Vigneron, D. B.; Larson, P. E. Z.; Harzstark, A. L.; Ferrone, M.; van Criekinge, M.; Chang, J. W.; Park, I.; et al. Metabolic Imaging of Patients with Prostate Cancer Using Hyperpolarized [1-^{13}C]Pyruvate. *Sci. Transl. Med.* **2013**, *5*, 198ra108.
(12) Keshari, K. R.; Wilson, D. M. Chemistry and Biochemistry of ^{13}C Hyperpolarized Magnetic Resonance Using Dynamic Nuclear Polarization. *Chem. Soc. Rev.* **2014**, *43*, 1627−1659.
(13) Kurhanewicz, J.; Vigneron, D. B.; Brindle, K.; Chekmenev, E. Y.; Comment, A.; Cunningham, C. H.; Deberardinis, R. J.; Green, G. G.; Leach, M. O.; Rajan, S. S.; et al. Analysis of Cancer Metabolism by Imaging Hyperpolarized Nuclei: Prospects for Translation to Clinical Research. *Neoplasia* **2011**, *13*, 81−97.
(14) Koptyug, I. V.; Kovtunov, K. V.; Burt, S. R.; Anwar, M. S.; Hilty, C.; Han, S. I.; Pines, A.; Sagdeev, R. Z. Para-Hydrogen-Induced Polarization in Heterogeneous Hydrogenation Reactions. *J. Am. Chem. Soc.* **2007**, *129*, 5580−5586.
(15) Bowers, C. R.; Weitekamp, D. P. Parahydrogen and Synthesis Allow Dramatically Enhanced Nuclear Alignment. *J. Am. Chem. Soc.* **1987**, *109*, 5541−5542.
(16) Adams, R. W.; Aguilar, J. A.; Atkinson, K. D.; Cowley, M. J.; Elliott, P. I. P.; Duckett, S. B.; Green, G. G. R.; Khazal, I. G.; López-Serrano, J.; Williamson, D. C. Reversible Interactions with Para-Hydrogen Enhance NMR Sensitivity by Polarization Transfer. *Science* **2009**, *323*, 1708−1711.
(17) Bowers, C. R.; Weitekamp, D. P. Transformation of Symmetrization Order to Nuclear-Spin Magnetization by Chemical Reaction and Nuclear Magnetic Resonance. *Phys. Rev. Lett.* **1986**, *57*, 2645−2648.
(18) Eisenschmid, T. C.; Kirss, R. U.; Deutsch, P. P.; Hommeltoft, S. I.; Eisenberg, R.; Bargon, J.; Lawler, R. G.; Balch, A. L. Para Hydrogen Induced Polarization in Hydrogenation Reactions. *J. Am. Chem. Soc.* **1987**, *109*, 8089−8091.
(19) Shchepin, R. V.; Coffey, A. M.; Waddell, K. W.; Chekmenev, E. Y. Parahydrogen Induced Polarization of 1-^{13}C-Phospholactate-d_2 for Biomedical Imaging with > 30,000,000-Fold NMR Signal Enhancement in Water. *Anal. Chem.* **2014**, *86*, 5601−5605.
(20) Zacharias, N. M.; Chan, H. R.; Sailasuta, N.; Ross, B. D.; Bhattacharya, P. Real-Time Molecular Imaging of Tricarboxylic Acid Cycle Metabolism in Vivo by Hyperpolarized 1-^{13}C Diethyl Succinate. *J. Am. Chem. Soc.* **2012**, *134*, 934−943.
(21) Shchepin, R. V.; Pham, W.; Chekmenev, E. Y. Dephosphorylation and Biodistribution of 1-^{13}C-Phospholactate in Vivo. *J. Labelled Compd. Radiopharm.* **2014**, *57*, 517−524.
(22) Shchepin, R. V.; Coffey, A. M.; Waddell, K. W.; Chekmenev, E. Y. PASADENA Hyperpolarized ^{13}C Phospholactate. *J. Am. Chem. Soc.* **2012**, *134*, 3957−3960.
(23) Coffey, A. M.; Shchepin, R. V.; Truong, M. L.; Wilkens, K.; Pham, W.; Chekmenev, E. Y. Open-Source Automated Parahydrogen Hyperpolarizer for Molecular Imaging Using ^{13}C Metabolic Contrast Agents. *Anal. Chem.* **2016**, *88*, 8279−8288.
(24) Hövener, J.-B.; Chekmenev, E. Y.; Harris, K. C.; Perman, W. H.; Tran, T. T.; Ross, B. D.; Bhattacharya, P. Quality Assurance of PASADENA Hyperpolarization for ^{13}C Biomolecules. *MAGMA* **2009**, *22*, 123−134.
(25) Bhattacharya, P.; Chekmenev, E. Y.; Reynolds, W. F.; Wagner, S.; Zacharias, N.; Chan, H. R.; Bunger, R.; Ross, B. D. Parahydrogen-Induced Polarization (PHIP) Hyperpolarized MR Receptor Imaging in Vivo: A Pilot Study of ^{13}C Imaging of Atheroma in Mice. *NMR Biomed.* **2011**, *24*, 1023−1028.
(26) Zhou, R.; Zhao, E. W.; Cheng, W.; Neal, L. M.; Zheng, H.; Quiñones, R. E.; Hagelin-Weaver, H. E.; Bowers, C. R. Parahydrogen-Induced Polarization by Pairwise Replacement Catalysis on Pt and Ir Nanoparticles. *J. Am. Chem. Soc.* **2015**, *137*, 1938−1946.
(27) Kovtunov, K. V.; Barskiy, D. A.; Salnikov, O. G.; Shchepin, R. V.; Coffey, A. M.; Kovtunova, L. M.; Bukhtiyarov, V. I.; Koptyug, I. V.; Chekmenev, E. Y. Toward Production of Pure ^{13}C Hyperpolarized Metabolites Using Heterogeneous Parahydrogen-Induced Polarization of Ethyl [1-^{13}C]Acetate. *RSC Adv.* **2016**, *6*, 69728−69732.
(28) Koptyug, I. V.; Zhivonitko, V. V.; Kovtunov, K. V. New Perspectives for Parahydrogen-Induced Polarization in Liquid Phase Heterogeneous Hydrogenation: An Aqueous Phase and ALTADENA Study. *ChemPhysChem* **2010**, *11*, 3086−3088.
(29) Kovtunov, K. V.; Zhivonitko, V. V.; Skovpin, I. V.; Barskiy, D. A.; Koptyug, I. V. Parahydrogen-Induced Polarization in Heterogeneous Catalytic Processes. *Top. Curr. Chem.* **2012**, *338*, 123−180.
(30) Gloggler, S.; Grunfeld, A. M.; Ertas, Y. N.; McCormick, J.; Wagner, S.; Schleker, P. P. M.; Bouchard, L. S. A Nanoparticle Catalyst for Heterogeneous Phase Para-Hydrogen-Induced Polarization in Water. *Angew. Chem., Int. Ed.* **2015**, *54*, 2452−2456.
(31) Goldman, M.; Jóhannesson, H. Conversion of a Proton Pair Para Order into C-13 Polarization by Rf Irradiation, for Use in MRI. *C. R. Phys.* **2005**, *6*, 575−581.
(32) Siddiqui, S.; Kadlecek, S.; Pourfathi, M.; Xin, Y.; Mannherz, W.; Hamedani, H.; Drachman, N.; Ruppert, K.; Clapp, J.; Rizi, R. The Use of Hyperpolarized Carbon-13 Magnetic Resonance for Molecular Imaging. *Adv. Drug Delivery Rev.* **2016**, DOI: 10.1016/j.addr.2016.08.011.
(33) Kadlecek, S.; Emami, K.; Ishii, M.; Rizi, R. Optimal Transfer of Spin-Order between a Singlet Nuclear Pair and a Heteronucleus. *J. Magn. Reson.* **2010**, *205*, 9−13.
(34) Haake, M.; Natterer, J.; Bargon, J. Efficient NMR Pulse Sequences to Transfer the Parahydrogen-Induced Polarization to Hetero Nuclei. *J. Am. Chem. Soc.* **1996**, *118*, 8688−8691.
(35) Bär, S.; Lange, T.; Leibfritz, D.; Hennig, J.; von Elverfeldt, D.; Hövener, J. On the Spin Order Transfer from Parahydrogen to Another Nucleus. *J. Magn. Reson.* **2012**, *225*, 25−35.
(36) Cai, C.; Coffey, A. M.; Shchepin, R. V.; Chekmenev, E. Y.; Waddell, K. W. Efficient Transformation of Parahydrogen Spin Order into Heteronuclear Magnetization. *J. Phys. Chem. B* **2013**, *117*, 1219−1224.
(37) Jóhannesson, H.; Axelsson, O.; Karlsson, M. Transfer of Para-Hydrogen Spin Order into Polarization by Diabatic Field Cycling. *C. R. Phys.* **2004**, *5*, 315−324.
(38) Reineri, F.; Boi, T.; Aime, S. Parahydrogen Induced Polarization of ^{13}C Carboxylate Resonance in Acetate and Pyruvate. *Nat. Commun.* **2015**, *6*, 5858.
(39) Kovtunov, K. V.; Barskiy, D. A.; Shchepin, R. V.; Salnikov, O. G.; Prosvirin, I. P.; Bukhtiyarov, A. V.; Kovtunova, L. M.; Bukhtiyarov, V. I.; Koptyug, I. V.; Chekmenev, E. Y. Production of Pure Aqueous ^{13}C-Hyperpolarized Acetate by Heterogeneous Parahydrogen-Induced Polarization. *Chem. - Eur. J.* **2016**, *22*, 16446−16449.
(40) Reineri, F.; Viale, A.; Ellena, S.; Alberti, D.; Boi, T.; Giovenzana, G. B.; Gobetto, R.; Premkumar, S. S. D.; Aime, S. ^{15}N Magnetic Resonance Hyperpolarization via the Reaction of Parahydrogen with ^{15}N-Propargylcholine. *J. Am. Chem. Soc.* **2012**, *134*, 11146−11152.
(41) Shchepin, R. V.; Barskiy, D. A.; Coffey, A. M.; Theis, T.; Shi, F.; Warren, W. S.; Goodson, B. M.; Chekmenev, E. Y. ^{15}N Hyperpolarization of Imidazole-$^{15}N_2$ for Magnetic Resonance pH Sensing via SABRE-SHEATH. *ACS Sensors* **2016**, *1*, 640−644.
(42) Jiang, W.; Lumata, L.; Chen, W.; Zhang, S.; Kovacs, Z.; Sherry, A. D.; Khemtong, C. Hyperpolarized ^{15}N-Pyridine Derivatives as pH-Sensitive MRI Agents. *Sci. Rep.* **2015**, *5*, 9104.
(43) Nonaka, H.; Hirano, M.; Imakura, Y.; Takakusagi, Y.; Ichikawa, K.; Sando, S. Design of a ^{15}N Molecular Unit to Achieve Long Retention of Hyperpolarized Spin State. *Sci. Rep.* **2017**, *7*, 40104.
(44) Nonaka, H.; Hata, R.; Doura, T.; Nishihara, T.; Kumagai, K.; Akakabe, M.; Tsuda, M.; Ichikawa, K.; Sando, S. A Platform for Designing Hyperpolarized Magnetic Resonance Chemical Probes. *Nat. Commun.* **2013**, *4*, 2411.
(45) Slichter, C. P. The Discovery and Demonstration of Dynamic Nuclear Polarization—a Personal and Historical Account. *Phys. Chem. Chem. Phys.* **2010**, *12*, 5741−5751.
(46) Wang, J.; Kreis, F.; Wright, A. J.; Hesketh, R. L.; Levitt, M. H.; Brindle, K. M. Dynamic ^{1}H Imaging of Hyperpolarized [1-^{13}C]Lactate In Vivo Using a Reverse INEPT Experiment. *Magn. Reson. Med.* **2017**, DOI: 10.1002/mrm.26725.

DOI: 10.1021/acs.jpcc.7b05912
J. Phys. Chem. C 2017, 121, 15304−15309

(47) Chekmenev, E. Y.; Norton, V. A.; Weitekamp, D. P.; Bhattacharya, P. Hyperpolarized ^{1}H NMR Employing Low Nucleus for Spin Polarization Storage. *J. Am. Chem. Soc.* **2009**, *131*, 3164−3165.
(48) Sarkar, R.; Comment, A.; Vasos, P. R.; Jannin, S.; Gruetter, R.; Bodenhausen, G.; Hall, H. H.; Kirik, D.; Denisov, V. P. Proton NMR of ^{15}N-Choline Metabolites Enhanced by Dynamic Nuclear Polarization. *J. Am. Chem. Soc.* **2009**, *131*, 16014−16015.
(49) Pfeilsticker, J. A.; Ollerenshaw, J. E.; Norton, V. A.; Weitekamp, D. P. A Selective ^{15}N-to-^{1}H Polarization Transfer Sequence for More Sensitive Detection of ^{15}N-Choline. *J. Magn. Reson.* **2010**, *205*, 125−129.
(50) Norton, V. A.; Weitekamp, D. P. Communication: Partial Polarization Transfer for Single-Scan Spectroscopy and Imaging. *J. Chem. Phys.* **2011**, *135*, 141107.
(51) Truong, M. L.; Coffey, A. M.; Shchepin, R. V.; Waddell, K. W.; Chekmenev, E. Y. Sub-Second Proton Imaging of ^{13}C Hyperpolarized Contrast Agents in Water. *Contrast Media Mol. Imaging* **2014**, *9*, 333−341.
(52) Mishkovsky, M.; Comment, A.; Gruetter, R. In Vivo Detection of Brain Krebs Cycle Intermediate by Hyperpolarized Magnetic Resonance. *J. Cereb. Blood Flow Metab.* **2012**, *32*, 2108−2113.
(53) Theis, T.; Ortiz, G. X.; Logan, A. W. J.; Claytor, K. E.; Feng, Y.; Huhn, W. P.; Blum, V.; Malcolmson, S. J.; Chekmenev, E. Y.; Wang, Q.; et al. Direct and Cost-Efficient Hyperpolarization of Long-Lived Nuclear Spin States on Universal $^{15}N_2$-Diazirine Molecular Tags. *Sci. Adv.* **2016**, *2*, e1501438−e1501438.
(54) Colell, J. F. P.; Logan, A. W. J.; Zhou, Z.; Shchepin, R. V.; Barskiy, D. A.; Ortiz, G. X.; Wang, Q.; Malcolmson, S. J.; Chekmenev, E. Y.; Warren, W. S.; et al. Generalizing, Extending, and Maximizing Nitrogen-15 Hyperpolarization Induced by Parahydrogen in Reversible Exchange. *J. Phys. Chem. C* **2017**, *121*, 6626−6634.
(55) Barskiy, D. A.; Salnikov, O. G.; Romanov, A. S.; Feldman, M. A.; Coffey, A. M.; Kovtunov, K. V.; Koptyug, I. V.; Chekmenev, E. Y. NMR Spin-Lock Induced Crossing (SLIC) Dispersion and Long-Lived Spin States of Gaseous Propane at Low Magnetic Field (0.05 T). *J. Magn. Reson.* **2017**, *276*, 78−85.
(56) Pravica, M. G.; Weitekamp, D. P. Net NMR Alignment by Adiabatic Transport of Parahydrogen Addition Products to High Magnetic Field. *Chem. Phys. Lett.* **1988**, *145*, 255−258.
(57) Golman, K.; Axelsson, O.; Johannesson, H.; Mansson, S.; Olofsson, C.; Petersson, J. S. Parahydrogen-Induced Polarization in Imaging: Subsecond ^{13}C Angiography. *Magn. Reson. Med.* **2001**, *46*, 1−5.
(58) Cavallari, E.; Carrera, C.; Boi, T.; Aime, S.; Reineri, F. Effects of Magnetic Field Cycle on the Polarization Transfer from Parahydrogen to Heteronuclei through Long-Range J-Couplings. *J. Phys. Chem. B* **2015**, *119*, 10035−10041.
(59) Shchepin, R. V.; Barskiy, D. A.; Coffey, A. M.; Esteve, I. V. M; Chekmenev, E. Y. Efficient Synthesis of Molecular Precursors for Para-Hydrogen-Induced Polarization of Ethyl Acetate-1-^{13}C and Beyond. *Angew. Chem., Int. Ed.* **2016**, *55*, 6071−6074.
(60) Kovtunov, K. V.; Barskiy, D. A.; Coffey, A. M.; Truong, M. L.; Salnikov, O. G.; Khudorozhkov, A. K.; Inozemtseva, E. A.; Prosvirin, I. P.; Bukhtiyarov, V. I.; Waddell, K. W.; et al. High-Resolution 3D Proton MRI of Hyperpolarized Gas Enabled by Parahydrogen and Rh/TiO_2 Heterogeneous Catalyst. *Chem. - Eur. J.* **2014**, *20*, 11636−11639.
(61) Kovtunov, K. V.; Barskiy, D. A.; Salnikov, O. G.; Burueva, D. B.; Khudorozhkov, A. K.; Bukhtiyarov, A. V.; Prosvirin, I. P.; Gerasimov, E. Y.; Bukhtiyarov, V. I.; Koptyug, I. V. Strong Metal-Support Interactions for Palladium Supported on TiO_2 Catalysts in the Heterogeneous Hydrogenation with Parahydrogen. *ChemCatChem* **2015**, *7*, 2581−2584.
(62) Burueva, D. B.; Salnikov, O. G.; Kovtunov, K. V.; Romanov, A. S.; Kovtunova, L. M.; Khudorozhkov, A. K.; Bukhtiyarov, A. V.; Prosvirin, I. P.; Bukhtiyarov, V. I.; Koptyug, I. V. Hydrogenation of Unsaturated Six-Membered Cyclic Hydrocarbons Studied by the Parahydrogen-Induced Polarization Technique. *J. Phys. Chem. C* **2016**, *120*, 13541−13548.
(63) Chekmenev, E. Y.; Hövener, J.-B.; Norton, V. A.; Harris, K.; Batchelder, L. S.; Bhattacharya, P.; Ross, B. D.; Weitekamp, D. P. PASADENA Hyperpolarization of Succinic Acid for MRI and NMR Spectroscopy. *J. Am. Chem. Soc.* **2008**, *130*, 4212−4213.
(64) Bhattacharya, P.; Chekmenev, E. Y.; Perman, W. H.; Harris, K. C.; Lin, A. P.; Norton, V. A.; Tan, C. T.; Ross, B. D.; Weitekamp, D. P. Towards Hyperpolarized ^{13}C-Succinate Imaging of Brain Cancer. *J. Magn. Reson.* **2007**, *186*, 150−155.
(65) Allouche-Arnon, H.; Lerche, M. H.; Karlsson, M.; Lenkinski, R. E.; Katz-Brull, R. Deuteration of a Molecular Probe for DNP Hyperpolarization - A New Approach and Validation for Choline Chloride. *Contrast Media Mol. Imaging* **2011**, *6*, 499−506.
(66) Shchepin, R. V.; Truong, M. L.; Theis, T.; Coffey, A. M.; Shi, F.; Waddell, K. W.; Warren, W. S.; Goodson, B. M.; Chekmenev, E. Y. Hyperpolarization of "Neat" Liquids by NMR Signal Amplification by Reversible Exchange. *J. Phys. Chem. Lett.* **2015**, *6*, 1961−1967.
(67) Barskiy, D. A.; Shchepin, R. V.; Coffey, A. M.; Theis, T.; Warren, W. S.; Goodson, B. M.; Chekmenev, E. Y. Over 20% ^{15}N Hyperpolarization in Under One Minute for Metronidazole, an Antibiotic and Hypoxia Probe. *J. Am. Chem. Soc.* **2016**, *138*, 8080−8083.
(68) Theis, T.; Truong, M. L.; Coffey, A. M.; Shchepin, R. V.; Waddell, K. W.; Shi, F.; Goodson, B. M.; Warren, W. S.; Chekmenev, E. Y. Microtesla SABRE Enables 10% Nitrogen-15 Nuclear Spin Polarization. *J. Am. Chem. Soc.* **2015**, *137*, 1404−1407.
(69) Sharma, U.; Baek, H. M.; Su, M. Y.; Jagannathan, N. R. In Vivo ^{1}H MRS in the Assessment of the Therapeutic Response of Breast Cancer Patients. *NMR Biomed.* **2011**, *24*, 700−711.
(70) Dorrius, M. D.; Pijnappel, R. M.; Jansen-van der Weide, M. C.; Jansen, L.; Kappert, P.; Oudkerk, M.; Sijens, P. E. Determination of Choline Concentration in Breast Lesions: Quantitative Multivoxel Proton MR Spectroscopy as a Promising Noninvasive Assessment Tool to Exclude Benign Lesions. *Radiology* **2011**, *259*, 695−703.
(71) Shchepin, R. V.; Chekmenev, E. Y. Synthetic Approach for Unsaturated Precursors for Parahydrogen Induced Polarization of Choline and Its Analogs. *J. Labelled Compd. Radiopharm.* **2013**, *56*, 655−662.

DOI: 10.1021/acs.jpcc.7b05912
J. Phys. Chem. C 2017, 121, 15304−15309